Interplay between soft and hard hadronic components for identified hadrons in relativistic heavy ion collisions

Tetsufumi Hirano[1,2] and Yasushi Nara[3]

[1]*Physics Department, University of Tokyo, Tokyo 113-0033, Japan*
[2]*RIKEN BNL Research Center, Brookhaven National Laboratory, Upton, New York 11973, USA*
[3]*Department of Physics, University of Arizona, Tucson, Arizona 85721, USA*

We investigate the transverse dynamics in Au+Au collisions at $\sqrt{s_{NN}}=200$ GeV by emphasis upon the interplay between soft and hard components through p_T dependences of particle spectra, ratios of yields, suppression factors, and elliptic flow for identified hadrons. From hydrodynamics combined with traversing minijets which go through jet quenching in the hot medium, we calculate interactions of hard jets with the soft hydrodynamic components. It is shown by the explicit dynamical calculations that the hydrodynamic radial flow and the jet quenching of hard jets are the keys to understand the differences among the hadron spectra for pions, kaons, and protons. This leads to the natural interpretation for $N_p/N_\pi \sim 1$, $R_{AA} \gtrsim 1$ for protons, and $v_2^p > v_2^\pi$ recently observed in the intermediate transverse momentum region at Relativistic Heavy Ion Collider.

I. INTRODUCTION

A vast body of data has already been collected and analyzed during the past few years at Relativistic Heavy Ion Collider (RHIC) [1] toward a complete understanding of the dense QCD matter which is created in high energy heavy-ion collisions.

At collider experiments, it is well known that high p_T perturbative QCD (pQCD) processes become so large as to observe jet spectra. One of the most important new physics revealed in heavy ion collisions at RHIC energies is to study propagation of (mini)jets in dense QCD matter. Jet quenching has been proposed [2] as a possible signal of deconfined nuclear matter, the quark gluon plasma (QGP) (for a recent review, see Ref. [3]). Over the past years, a lot of work has been devoted to study the propagation of jets through QCD matter [4–7].

Recent data at RHIC indicate that both the neutral pion [8,9] and the charged hadron [10–12] spectra at high p_T in central Au+Au collisions are suppressed relative to the scaled pp or large centrality spectra by the number of binary collisions. However, protons do not seem to be quenched in the moderate p_T range [13]. Furthermore, the proton yield exceeds the pion yield around $p_T \sim 2-3$ GeV/c which is not seen in elementary hadronic collisions [12]. The STAR Collaboration also shows that $\Lambda/K^0 \sim 1$ at a transverse momentum of $2-3$ GeV/c [14]. pQCD calculations are successful in describing hadron spectra in Au+Au collisions as well as pp collisions by taking account of nuclear effects such as Cronin effect, nuclear shadowing effect, and energy loss of jets [15]. However, large uncertainty of the proton fragmentation function makes the understanding of the baryon production mechanism unclear [16] even in pp collisions. On the other hand, several models have been proposed by considering interplay between nonperturbative soft physics and pQCD hard physics: baryon junction [17,18], parton coalescence [19–23], medium modification of the string fragmentation [24], and a parametrization with hydrodynamic com-

ponent combined with the nonthermal components [25] in order to explain the anomalous baryon productions and/or large elliptic flow discovered at RHIC.

It is said that hydrodynamics [26–29] works very well for explanation of elliptic flow data at RHIC energies, in the low p_T region, in small centrality events, and at midrapidity, including the mass dependence of hadrons (for recent reviews, see Ref. [30]). This suggests that hydrodynamics could be reliable for the description of the time evolution of soft sector of matter produced in high energy heavy-ion collisions at RHIC. Certainly, it is more desirable to describe the time evolution of the whole stage in high energy heavy-ion collisions by simulating collisions of initial nuclear wave functions. Instead, they simply assume that the system created in heavy-ion collisions reaches local thermal equilibrium state at some time.

Due to the above two reasons, a model which treats a soft sector by hydrodynamics and a hard sector based on a pQCD parton model is turned out to be useful in order to understand experimental data at RHIC *from low to high p_T*. Indeed, first attempts based on this concept has been done by pQCD calculations which include hydrodynamic features [31–33]. Motivated by these works, we have recently developed a two component *dynamical* model (hydro+jet model) [34] with a fully three-dimensional hydrodynamic model [28] for the soft sector and pQCD jets for the hard sector which are computed via the PYTHIA code [35].

Usually, it is possible to fit hadron spectra up to high momentum, say $p_T \sim 2-3$ GeV/c, within hydrodynamics by adjusting kinetic freeze-out temperature T^{th} which is a free parameter in the model [36]. Thus it is unclear which value of Tth should be used when one wants to add jet components into hydrodynamic components for the description of high p_T part. However, we are free from this problem thanks to inclusion of the early chemical freeze-out picture into hydrodynamics. One of the authors studied the effects of chemical freeze-out temperature T^{ch} which is separate from kinetic one T^{th} in hydrodynamic model in Ref. [29]. It was found that the

p_T slope for pions remains invariant under the variation of Tth and that the hydrodynamic model with early chemical freeze out is able to fit the transverse momentum distribution of pions up to $1-2$ GeV/c. Therefore, it is certain to incorporate hard partons into the hydrodynamics with early freeze out in order to account for the high transverse momentum part of the hadronic spectrum. We note that, since we do not assume thermalization for the high p_T jets, a hydrodynamical calculation with the initial conditions taken from pQCD +final state saturation model [37] is different from ours.

In this paper, we shall study identified hadron spectra from low to high p_T within the hydro+jet model. In particular, we focus on the influence of the hydrodynamic radial flow on the pQCD predictions for the transverse spectra. Parameters in the hydrodynamic part of the model have been already fixed by fitting the pseudorapidity distribution. Parameters related to the propagation of partons are also obtained by fitting the neutral pion suppression factor by PHENIX and are found to be consistent [38] with the back-to-back correlation data from STAR [39].

The paper is organized as follows. In Sec. II, we describe the main features of our model. We will represent results of transverse momentum distributions for pions, kaons, and protons in Sec. III A. Nuclear modification factor (suppression factor) for identified hadrons and particle ratios are discussed in Sec. III B. Elliptic flow for identified hadrons is discussed in Sec. III C. Section IV summarizes this paper.

II. MODEL DESCRIPTION

In this section, we explain in some detail the hydro+jet model as a dynamical model to describe relativistic heavy ion collisions.

A. Hydrodynamics

Let us start with the review of our hydrodynamics. Main features of the hydrodynamic part in the hydro+jet model are the following.

Although initial conditions and prethermalization stages are very important subjects in the physics of heavy ion collisions (see, e.g., Refs. [40,41]), these are beyond the scope of this paper. Instead, assuming local thermal equilibrium of partonic/hadronic matter at an initial time τ_0, we describe afterward the space-time evolution of thermalized matter by solving the equations for energy-momentum conservation

$$\partial_\mu T^{\mu\nu} = 0, \quad T^{\mu\nu} = (e+P)u^\mu u^\nu - Pg^{\mu\nu} \quad (1)$$

in the *full* three-dimensional Bjorken coordinate (τ, x, y, η_s). Here e, P, and u^μ are, respectively, energy density, pressure, and local four velocity. $\tau = \sqrt{t^2 - z^2}$ is the proper time and $\eta_s = (1/2)\ln[(t+z)/(t-z)]$ is the space-time rapidity. Throughout this paper, we consider baryon free matter $n_B = 0$ at RHIC energies. In order to obtain reliable solutions of Eq. (1) especially in the longitudinal direction at collider energies, τ and η_s are substantial choices for time and longitudinal directions rather than the Cartesian coordinate.

Assuming $N_f = 3$ massless partonic gas for the QGP phase, an ideal gas equation of state with a bag constant $B^{1/4} = 247$ MeV is used in the high temperature phase. We use a hadronic resonance gas model with all hadrons up to $\Delta(1232)$ for later stages of collisions. Possible finite baryonic effects such as a repulsive mean field [42] are not included because of the low baryon density at RHIC [43]. Phase transition temperature is set to be $T_c = 170$ MeV. For the hadronic phase, a partial chemical equilibrium model with chemical freeze-out temperature $T^{ch} = 170$ MeV is employed to describe the early chemical freeze-out picture of hadronic matter. Although chemical freeze-out temperature $T^{ch}(\sim 160-170$ MeV$)$ is usually found to be larger than kinetic freeze-out temperature $T^{th}(\sim 100-140$ MeV$)$ from statistical model analyses and thermal model fitting [44], the sequential freeze out is not considered so far in the conventional hydrodynamics except for a few work [29,45–47]. As a consequence of this improvement, the hadron phase cools down more rapidly than the one in usual hydrodynamic calculations in which $T^{ch} = T^{th}$ is assumed [29,45]. It should be emphasized that the slope of pions in the transverse momentum distribution becomes insensitive to the choice of the kinetic freeze-out temperature T^{th} and that the hydrodynamics with early chemical freeze out reproduces the RHIC data of the pion transverse momentum only up to 1.5 GeV/c [48]. This is one of the strong motivations which leads us to combine our hydrodynamics with nonthermalized hard components.

From hydrodynamic simulations, we evaluate hadronic spectra which originate from thermalized hadronic matter. For hadrons directly emitted from freeze-out hypersurface Σ, we calculate spectra through the Cooper-Frye formula [49]

$$E\frac{dN_i}{d^3p} = \frac{d_i}{(2\pi)^3}\int_\Sigma \frac{p^\mu d\sigma_\mu}{\exp[(p^\mu u_\mu - \mu_i)/T^{th}] \mp 1}, \quad (2)$$

where d_i is a degeneracy factor, μ_i is a chemical potential, p^μ is a four-momentum in the center of mass frame of colliding two nuclei, and $-(+)$ sign is taken for bosons (fermions). We should note the existence of chemical potentials μ_i for *all* hadrons under consideration due to early chemical freeze out. Typical values at $T^{th} = 100$ MeV are as follows: $\mu_\pi = 83$ MeV, $\mu_K = 181$ MeV, and $\mu_p = \mu_{\bar{p}} = 349$ MeV. For hadrons from resonance decays, we use Eq. (2) for resonance particles at freeze out and afterward take account of decay kinematics. Here these resonances also have their own chemical potentials at freeze out. We call the sum of the above spectra the soft component or the hydro component throughout this paper.

Initial energy density at $\tau_0 = 0.6$ fm/c is assumed to be factorized

$$e(x,y,\eta_s;b) = e_{max}W(x,y;b)H(\eta_s). \quad (3)$$

Here the transverse profile $W(x,y;b)$ is proportional to the number of binary collisions and normalized as $W(0,0;0) = 1$, whereas longitudinal profile $H(\eta_s)$ is flat and unity near midrapidity and falls off smoothly at large rapidity. In $H(\eta_s)$, we have two adjustable parameters η_{flat} and η_{Gauss} which parametrize the length of flat region near midrapidity and
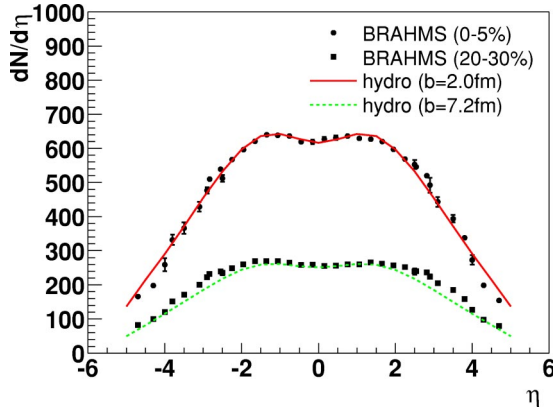
FIG. 1. (Color online) Pseudorapidity distribution of charged particles in Au+Au collisions at $\sqrt{s_{NN}}$=200 GeV is compared to data from BRAHMS [50]. Solid (dashed) line represents the hydrodynamic result at b=2.0 (7.2)fm.

the width of Gaussian in the forward/backward rapidity region, respectively. These parameters are chosen so as to reproduce the shape of $dN/d\eta$ or dN/dY.

We choose e_{max}=40 GeV/fm^3, η_{flat}=4.0, and η_{Gauss}=0.8. As shown in Fig. 1, the pseudorapidity distribution of charged hadrons in 5 % central collisions observed by the BRAHMS Collaboration [50] is satisfactory reproduced by using the above parameters. Here we choose an impact parameter as b=2 fm for this centrality. These initial parameters give us an average initial energy density about 5 GeV/fm^3 in the transverse plane η_s=0 at τ=1 fm/c [51]. A contribution from minijets is neglected in the hydrodynamic fitting, since it is less than 5 % effect to the total hadron yield at RHIC when we define minijets as particles with transverse momentum larger than 2 GeV/c. Initial conditions for transverse profile are scaled by the number of binary collisions. It is found that the 20–30 % semicentral collision data is also reproduced simply by choosing b as 7.2 fm in the transverse profile W [52].

In Fig. 2, we show the transverse spectra for negative pions, negative kaons, and protons in Au+Au collisions at $\sqrt{s_{NN}}$=200 GeV from the hydrodynamic model for impact parameters b=2.0 fm and 7.2 fm. Thermal freeze-out temperature T^{th}=100 MeV is used in the calculation. This choice is consistent with the data at $\sqrt{s_{NN}}$=130 GeV [29]. The flatter behavior at low p_T for kaons and protons is indeed a consequence of the radial flow effect. A remarkable feature on the hydrodynamical result is that $p/\pi^->1$ and $K^-/\pi^-\sim1$ above $p_T\sim2$ GeV/c. It is, however, questionable to assume thermalization at high p_T region. In fact, hydrodynamical predictions overestimate elliptic flow data at the large transverse momentum region. It is interesting to ask at which p_T hydrodynamic behavior ceases and switches to pQCD results. We will see in the following section how these hydrodynamical results are modified by including the pQCD hard component.

B. Jet propagations

For the hard part of the model, we generate hard partons according to a pQCD parton model. The number of jets at an impact parameter $\boldsymbol{b}$ are calculated from
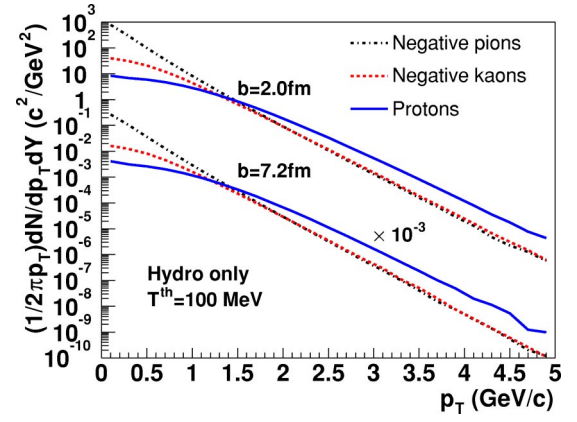

FIG. 2. (Color online) Transverse momentum spectra for negative pions, negative kaons, and protons from the hydro model with early chemical freeze out in Au+Au collisions at $\sqrt{s_{NN}}$=200 GeV. We choose an impact parameter as b=2.0 (7.2)fm corresponding to 0–5 % (20–30 %) centrality. Yields are divided by 10^3 for b=7.2 fm results.

$$N_{hard}(\boldsymbol{b}) = \int d^2\boldsymbol{r}_\perp \sigma_{jet} T_A(\boldsymbol{r}_\perp - \boldsymbol{b}/2)T_B(\boldsymbol{r}_\perp + \boldsymbol{b}/2), \quad (4)$$

where σ_{jet} is a hard cross section from leading order pQCD convoluted by the parton distribution functions and multiplied by a K factor which takes into account higher order contributions. T_A and $\boldsymbol{r}_\perp$ are, respectively, a nuclear thickness function normalized to be $\int d^2\boldsymbol{r}_\perp T_A=A$ and a transverse coordinate vector. Here we use the Woods-Saxon distribution for the nuclear density profile. We use PYTHIA 6.2 [35] for the generation of momentum spectrum of jets through $2\rightarrow2$ QCD hard processes. Initial and final state radiations are used to take into account the enhancement of higher-order contributions associated with multiple small-angle parton emission.

Scale Q^2 dependent nuclear shadowing effect is included for the mass number A nucleus assuming the impact parameter dependence [53]:

$$S(A,x,Q^2,\boldsymbol{r}_\perp) = 1 + [S(A,x,Q^2) - 1]\frac{AT_A(\boldsymbol{r}_\perp)}{\int d^2\boldsymbol{r}_\perp T_A(\boldsymbol{r}_\perp)^2}, \quad (5)$$

where the EKS98 parametrization [54] is used for $S(A,x,Q^2)$. Then the nuclear parton distribution function in this model has the form

$$f_A(A,x,Q^2,\boldsymbol{r}_\perp) = S(A,x,Q^2,\boldsymbol{r}_\perp)$$
$$\times \left[\frac{Z}{A}f_p(x,Q^2) + \frac{(A-Z)}{A}f_n(x,Q^2)\right], \quad (6)$$

where $f_p(x,Q^2)$ and $f_n(x,Q^2)$ are the parton distribution functions for protons and neutrons. We simply assume the charge of a nucleus to be $Z=A/2$ in consistency with the soft part, since our fluids are assumed to be isospin symmetric as well as baryon free matter.

Cronin effect [55], which has also been discovered in recent RHIC experiments [56], is usually considered as the

multiple initial state scattering effect. Understanding this effect becomes an important subject in RHIC physics [57–59]. We employ the model in Ref. [57] to take into account the multiple initial state scatterings, in which initial k_T is broadened proportional to the number of scatterings:

$$\langle k_T^2 \rangle_{NA} = \langle k_T^2 \rangle_{NN} + \delta^2(Q^2)[\sigma_{NN} T_A(\mathbf{r}_\perp) - 1], \tag{7}$$

where σ_{NN} is the inelastic nucleon-nucleon cross section and $\delta^2(Q^2)$ is the scale dependent k_T broadening per nucleon-nucleon collision whose explicit form can be found in Ref. [57].

We need to specify a scale which separates a soft sector from a hard sector, in other words, a thermalized part from a nonthermalized part in our model. We include minijets with transverse momentum $p_{T,\text{jet}}$ larger than 2 GeV/c just after hard scatterings in the simulation. These minijets explicitly propagate through fluid elements.

Since we only pick up high p_T partons from PYTHIA and throw them into fluids, there is ambiguity to connect color flow among partons. Thus we use an independent fragmentation model option in PYTHIA to convert hard parton to hadrons instead of using the default Lund string fragmentation model. We note that the independent fragmentation model should not be applied at low transverse momentum region. We have checked that the neutral pion transverse spectrum in pp collisions at RHIC [60] is well reproduced by selecting the K factor $K=2.5$, the scale $Q=p_{T,\text{jet}}/2$ in the CTEQ5 leading order parton distribution function [61], and the primordial transverse momentum $\langle k_T^2 \rangle_{NN}=1$ GeV$^2/c^2$ as shown in Fig. 3. As shown in the bottom panel of the Fig. 3, independent fragmentation model predictions for pions and kaons are very close to those from the Lund string fragmentation model in $p_T > 2$ GeV/c, where $K=2$ and $Q=p_{T,\text{jet}}/2$ is used in the Lund string model case and non-perturbative inelastic soft processes are included. However, the yield of protons from the independent fragmentation scheme becomes much less than that from Lund string model predictions as seen in Fig. 3. We found that the Lund fragmentation scheme is favored in terms of the recent STAR data of protons in pp collisions [62]. In what follows, we make corrections for our p_T spectra of kaons and protons in Au+Au collisions according to the result in the bottom panel of Fig. 3.

In order to see the theoretical uncertainties on the fragmentation scheme deeply, we also plot the results from NLOpQCD calculations [63] with the MRST99 [64] set of parton distribution functions. In Fig. 3, we show results from two different fragmentation functions. The solid lines are obtained from Kniehl-Kramer-Potter (KKP) fragmentation functions [65] with renormalization scale μ, factorization scale M, and fragmentation scale M_f equal to p_T. NLOpQCD prediction with KKP fragmentation functions is consistent with the pion data. NLOpQCD predictions with the Kretzer fragmentation functions [66] assuming $\mu=M=M_F=p_T/2$ underestimate pion yields, while yields for kaons and protons are the same as the predictions from the PYTHIA default Lund string fragmentation model.
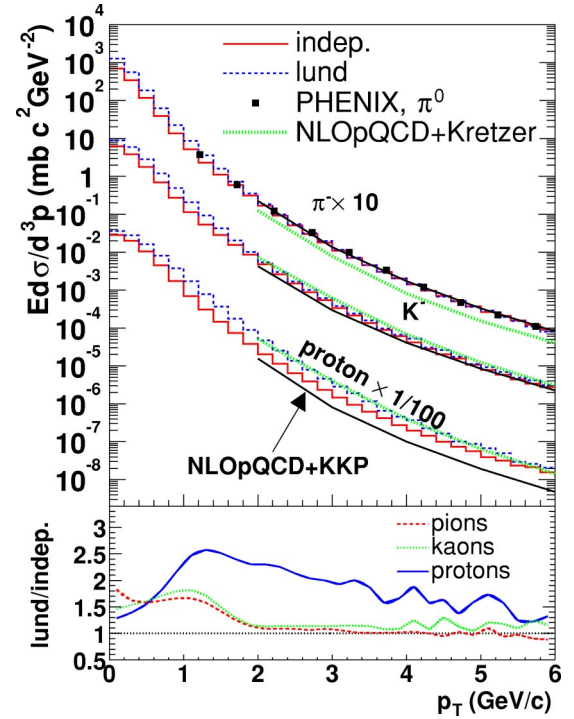

FIG. 3. (Color online) Comparison with various models for inclusive pion, kaon, and proton transverse momentum distributions in pp collisions at $\sqrt{s}=200$ GeV. Solid and dotted histograms correspond to the results from PYTHIA with independent fragmentation, and default Lund fragmentation, respectively. Solid and dotted lines are, respectively, from NLOpQCD calculations with KKP and Kretzer fragmentation functions.

Initial transverse positions of jets at an impact parameter $\mathbf{b}$ are determined randomly according to the probability $P(\mathbf{r}_\perp, \mathbf{b})$ specified by the number of binary collision distribution,

$$P(\mathbf{r}_\perp, \mathbf{b}) \propto T_A(\mathbf{r}_\perp + \mathbf{b}/2) T_A(\mathbf{r}_\perp - \mathbf{b}/2). \tag{8}$$

Initial longitudinal position of a parton is approximated by the boost invariant distribution [67]: $\eta_s = Y$, where $Y = (1/2)\ln[(E+p_z)/(E-p_z)]$ is the rapidity of a parton. Jets are freely propagated up to the initial time τ_0 of hydrodynamic simulations by neglecting the possible interactions in the prethermalization stages. Jets are assumed to travel with straight line trajectory in a time step:

$$\Delta r_i = \frac{p_i}{m_T \cosh(Y - \eta_s)} \Delta \tau, \quad (i=x,y), \tag{9}$$

$$\Delta \eta_s = \frac{1}{\tau} \tanh(Y - \eta_s) \Delta \tau, \tag{10}$$

where $m_T = \sqrt{m^2 + p_T^2}$ is a transverse mass.

Jets can suffer interaction with fluids and lose their energies. We employ the approximate first order formula [Gyulassy-Levai-Vitev (GLV) formula] in opacity expansion from the reaction operator approach [7] for the energy loss of partons throughout this work. The opacity expansion is rel-
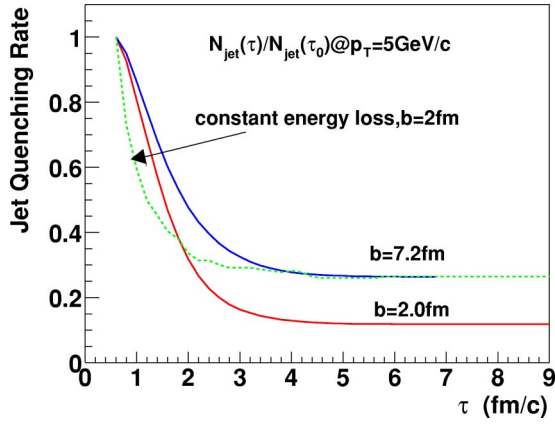
FIG. 4. (Color online) Jet quenching rate $N_{jet}(\tau)/N_{jet}(\tau_0)$ for $p_T=5$ GeV/c jets in Au+Au collisions at $\sqrt{s_{NN}}=200$ GeV. Jet quenching rate for 10 GeV/c jets is very similar to that of the 5 GeV/c jets.

evant for the realistic heavy ion reactions where the number of jet scatterings is small. The energy loss formula for coherent scatterings in matter has been applied to analysis of heavy-ion reactions taking into account the expansion of the system [15,31–33]. The approximate first order formula in this approach can be written as

$$\Delta E = C \int_{\tau_0}^{\infty} d\tau \rho(\tau,\boldsymbol{x}(\tau))(\tau - \tau_0)\ln\left(\frac{2E_0}{\mu^2 L}\right). \quad (11)$$

Here C is an adjustable parameter and $\rho(\tau,\boldsymbol{x})$ is a thermalized parton density in the local rest frame of fluid elements in the hydro+jet approach [68]. $\boldsymbol{x}(\tau)$ and E_0 are the position and the initial energy of a jet, respectively. The initial energy E_0 in Eq. (11) is Lorentz-boosted by the flow velocity and replaced by $p_0^\mu u_\mu$ where p_0^μ is the initial four momentum of a jet and u_μ is a local fluid velocity. We take a typical screening scale $\mu=0.5$ GeV and effective path length $L=3$ fm which is chosen from the lifetime of the QGP phase. Here we choose $C=0.45$ [69] which is found to reproduce the neutral pion R_{AA} defined by Eq. (12) [9]. Our purpose here is not a detailed study of jet quenching mechanisms. Instead, we first fit the suppression factor for neutral pions and next see other hadronic spectra.

Feedback of the energy to fluid elements in central collisions was found to be about 2% of the total fluid energy. Hence we can safely neglect its effect on hydrodynamic evolution in the case of the appropriate amount of energy loss.

In Fig. 4, we show the jet quenching rate as a function of proper time for 5 GeV/c jets. We count the number of partons with $4.5<p_{T,jet}<5.5$ GeV/c at each time step, and then define the ratio of the current number of jets to the initial number of jets $N_{jet}(\tau)/N_{jet}(\tau_0)$. Most jet quenching is completed at early times less than 4 fm/c. For comparison, we also plot the jet quenching rate for a constant energy loss case $dE/dx \propto \rho(\tau)$. Jet quenching is almost finished at $\tau \sim 2$ fm/c in the case of constant energy loss. From Fig. 4, the degree of decrease for the jet quenching rate in the GLV formula becomes milder and continues longer than that in the

incoherent model. This is due to the existence of τ in the integrand in Eq. (11) which comes from the property of coherent (Landau-Pomeranchuk-Migdal [70]) effect. Contrary to the simple Bjorken's ansatz [67], $\rho(\tau)=\rho_0\tau_0/\tau$, there exists transverse flow and the parton density profile in the transverse plane is not flat in our simulations. This is the reason why jets are quenched only in the QGP phase and why jet quenching in the mixed phase is totally negligible.

We include $p_\perp$ broadening accompanied by the energy loss of jets with the formula $\langle p_\perp^2 \rangle \sim \int d\tau \rho(\boldsymbol{r})$ as in Ref. [38]. We found that this effect is small in all results in this paper.

Within our model, we neglect energy loss before thermalization, in our case, $\tau<0.6$ fm/c. One would ask if it is important to take into account the energy loss effects before thermalization because parton density has the maximum value. We can, however, fit the suppression factor R_{AA} by rescaling the energy loss parameter C when the initial time τ_0 is changed. The question about the jet quenching before thermalization is beyond our model description. As a possible model for a study of jet interactions at early times, propagation of jets in the classical Yang-Mills fields based on the idea of the color glass condensate [40,71] is proposed in Ref. [72]. It would be interesting to take numerical results from the full lattice calculations [73] for the calculations of jet energy loss at the very early stages of the collisions.

III. RESULTS

We discuss in this section transverse dynamics for pions, kaons, and protons from the hydro+jet model focusing on the intermediate p_T where interplay between soft and hard components is expected to be crucial. As mentioned in the preceding section, a parameter for jet quenching C was already fixed by fitting the observed data for neutral pions in central Au+Au collisions from PHENIX. Freeze-out temperature $T^{th}=100$ MeV is used for hydrodynamics. All results in this section are for midrapidity $|\eta|<0.35$.

A. Transverse momentum distributions for identified particles

First, we show the transverse momentum distributions for pions, kaons, and protons from the hydro+jet model in Fig. 5 in central as well as semicentral Au+Au collisions at RHIC. Each spectrum is the sum of the soft component and the hard component. Before summation, the hard component is multiplied by a "switch" function [31] $\{1+\tanh[2(p_T-p_{T,cut})]\}/2$ (where p_T is in the unit of GeV/c and $p_{T,cut}=2$ GeV/c) in order to cut the unreliable components from the independent fragmentation scheme and also to fit R_{AA} for neutral pions [9]. We have checked the cutoff parameter dependence in the switch function on the pion spectrum and found that we are not able to fit the pion data anymore even with $p_{T,cut}=1.8$ or 2.2 GeV/c. So the ambiguity of the cut off can be removed to fit the pion data within our approach.

At low transverse momentum region $p_T<1$ GeV/c, the shapes remain the same as hydro predictions as one can check from Fig. 2. Also at high transverse momentum, spectra are identical to those of pQCD predictions with an appropriate amount of jet quenching.
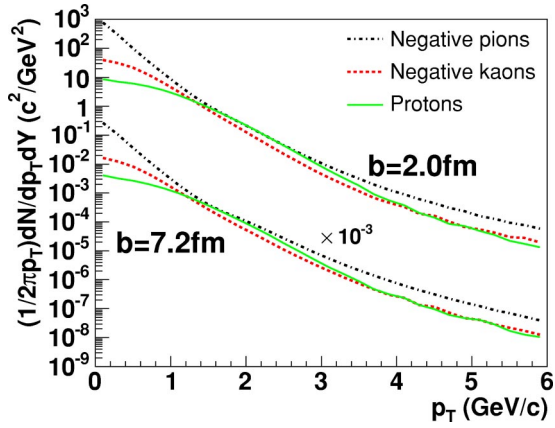
FIG. 5. (Color online) Transverse momentum spectra for negative pions, negative kaons, and protons from the hydro+jet model in Au+Au collisions at $\sqrt{s_{NN}}=200$ GeV at the impact parameter of $b=2.0$ and 7.2 fm. Yields are divided by 10^3 for $b=7.2$ fm results.

Our calculation includes interactions of minijets with QGP fluids. We also note that there remains a pQCD-like power law behavior in all hadrons at high transverse momentum. This may indicate no hint for the thermalization at high transverse momentum. However, energy loss results in a parallel shift of hadronic spectra, since the energy loss model used in this paper shows almost flat quenching pattern as shown in our previous analysis [38].

In Fig. 6, we decompose the spectra into hydro parts and minijet parts. Here the yields from hard components are multiplied by the switch function again. It is seen that both soft and hard components are important for the hadron spectra in the transverse momentum of the range around $2 \lesssim p_T \lesssim 5$ GeV/c depending on the hadron mass. We can define the crossing point of transverse momentum $p_{T,cross}$ at which the yield from the soft part is identical to that from the hard part. $p_{T,cross}$ moves toward high momentum with mass of particles because of the effects of radial flow. In central collisions, $p_{T,cross} \sim 1.8$, 2.5, and 3.5 GeV/c for pions, kaons, and protons, respectively. Minijet spectra are recovered at $p_T \sim 3.4$ GeV/c for pions, $p_T \sim 4.0$ GeV/c for kaons, and $p_T \sim 5.0$ GeV/c for protons.

We give some remarks as follows:

(i) The point at which hydrodynamic and pQCD spectra cross is determined by the dynamics of the system. The radial flow pushes the soft components toward high p_T region, while the dense matter reduces the pQCD components through parton energy loss. The crossing of two spectra causes by interplay of these two effects.

(ii) At $p_T=2-3$ GeV/c, the yields of pions and kaons are no longer occupied by soft hydrodynamic component. On the other hand, the proton yield from pQCD prediction is about ten times smaller than that of hydro in the transverse momentum region.

(iii) One may try to extract the strength of radial flow and the kinetic freeze-out temperature from experimental data through the hydrodynamics-motivated fitting model. Then one should pay attention to the fitting range of the transverse momentum. In particular, p_T spectrum for pions may have no room to fit by a simple thermal spectrum: Contribution from
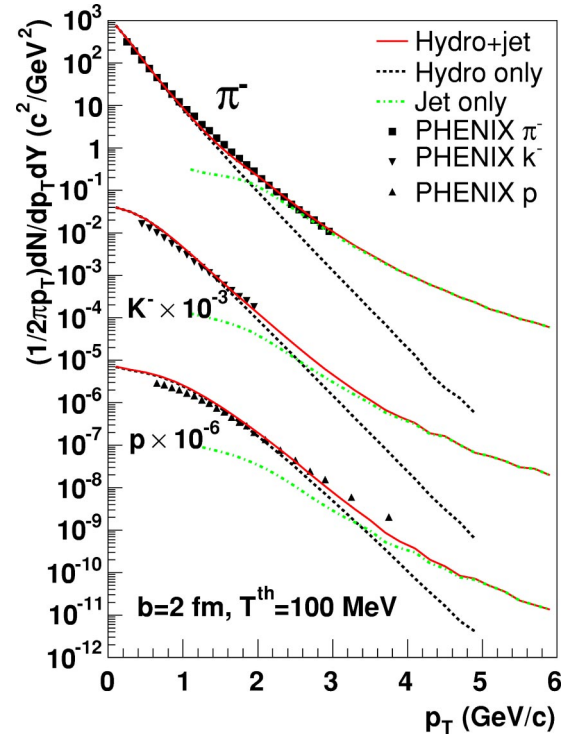

FIG. 6. (Color online) Each contribution from hydrodynamics and minijets for π^-, K^-, and p in Au+Au collisions at $\sqrt{s_{NN}}=200$ GeV at the impact parameter of $b=2.0$ fm. Yield of negative kaons (protons) is divided by 10^3 (10^6). PHENIX data are from Ref. [74].

resonance decays becomes important below $p_T \sim 0.5$ GeV/c, while the hard component slides in the soft component near $p_T \sim 1.0$ GeV/c.

(iv) We predict positions of the inflection point where p_T spectrum becomes convex to concave: $p_T \sim 3$ GeV/c for kaons and ~ 4 GeV/c for protons. These are the indicators of a transition from soft physics to hard physics.

The amount of the hydrodynamic contributions to the hadron yields for each particle found in the hydro+jet model is very similar to that found in Ref. [25] in which hybrid parametrization of hydrodynamics with the spectral shape in pp collisions. It is also remarkable that baryon junction [17,18] and quark coalescence models [20–22] predicts the same behavior. Quark coalescence models are successful in explaining the mass dependence of p_T slopes [75,76]. For example, one can easily understand the difference of the transverse slopes of baryons and mesons from a quark coalescence hadronization mechanism. A baryon momentum is a sum of three quarks (quark momenta must be almost parallel in order to cluster), but a momentum of mesons is a sum of two quarks. It is interesting to see, for example, ϕ meson spectrum in order to distinguish the mass effects in hydrodynamics from meson-baryon effects in coalescence models.

B. Suppression factors and particle ratios

We now turn to the study of the suppression factors R_{AA} for each hadron defined by
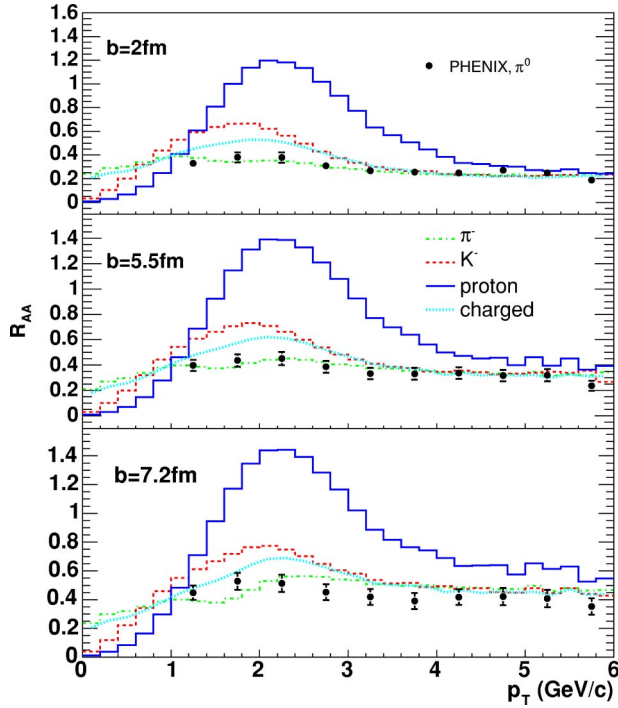
FIG. 7. (Color online) Impact parameter dependence of the suppression factors R_{AA} in Au+Au collisions at $\sqrt{s_{NN}}=200$ GeV as a function of p_T for π^-, K^-, and p. R_{AA} for charged hadrons is also shown in dotted lines. Experimental data of R_{AA} for neutral pions [9] is obtained by PHENIX. For details, see text.

$$R_{AA} = \frac{\dfrac{dN^{A+A}}{d^2p_T dY}}{N_{\text{coll}}\dfrac{dN^{p+p}}{d^2p_T dY}}. \tag{12}$$

It is very instructive to study R_{AA} behaviors for identified hadrons toward a comprehensive understanding of intermediate transverse momentum region.

Figure 7 shows the suppression factors R_{AA} for pions, kaons, protons, and charged hadrons respectively in Au+Au collisions at RHIC for impact parameters $b=2.0$, 5.5, and 7.2 fm. Our results for pions are compared with PHENIX data [9]. We use pp spectra from Lund string model for protons and kaons in the plots. R_{AA} for protons using the independent fragmentation model becomes too large ~ 2.5 at $p_T \sim 2$ GeV/c. This result simply comes from the fact that the independent fragmentation model is inconsistent with pp data for protons as discussed in Sec. II. Note that the numerator in Eq. (12) is almost free from the hard components at $p_T < 3$ GeV/c in proton case. We find protons are not suppressed $R_{AA} > 1$ at a momentum range of $1.5 < p_T < 2.5$ GeV/c. Pions, on the contrary, are largely suppressed for all momentum range. Our calculations for protons become identical to those of pQCD predictions at a momentum above 5 GeV/c. This is the same result as other model predictions [21,22,25]. In any case, these results are easily understood from Fig. 6: The crossing point $p_{T,\text{cross}}$ depends on the hadronic species, thus R_{AA} only for pions
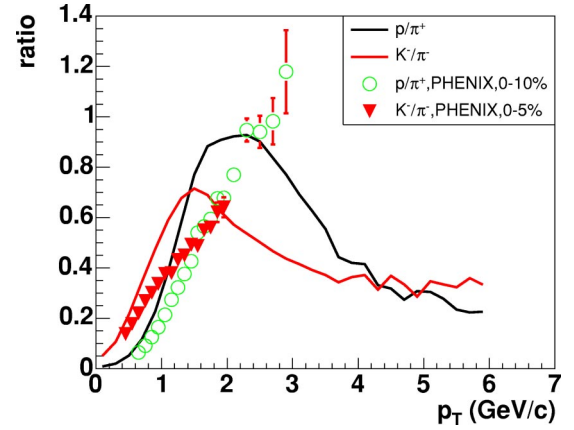

FIG. 8. (Color online) Ratios of N_p to N_{π^-} and N_{K^-} to N_{π^-} as a function of p_T in Au+Au collisions at impact parameter $b=2$ fm. PHENIX data [74] are also ploted for comparsion.

reflects jet quenching effect, while the larger value of R_{AA} for protons simply comes from radial flow, not the absence of jet quenching. We should mention that above $p_T \sim 5$ GeV/c, suppression factors for identified hadrons converge to almost the same value. It is also seen that the suppression factors for kaons and protons have almost no centrality dependence within this impact parameter range.

Recent data from PHENIX [13] and STAR [14] for protons and Λ's show that the nuclear modification factors for p, $\bar{p}$, and Λ in the p_T range of $1.5 < p_T < 4.5$ GeV/c are almost constant. However, our results of R_{AA} for protons seem to decrease to smaller value with transverse momentum faster than data.

From RHIC data [8–11], R_{AA} for charged particles is larger than the one for pions in moderate high p_T region. In our model, this also simply results from the average of the above three suppression factors weighted by each yield (see also Fig. 5) as shown in Fig. 7 by the dotted lines.

We show in Fig. 8 proton to negative pion ratio and negative kaon to negative pion ratios as a function of the transverse momentum in Au+Au collisions at $\sqrt{s_{NN}}=200$ GeV for the impact parameter of $b=2$ fm together with the PHENIX data [74]. Without depending on baryon junction mechanism or quark coalescence models, we also obtain that p/π^- ratio becomes close to unity due to the consequences of hadron species dependent $p_{T,\text{cross}}$. Ratios become $p/\pi^- \sim 0.2$ and $K^-/\pi^- \sim 0.3$ above $p_T \sim 5$ GeV/c which are the consequences of pQCD predictions. It should be noted that, if the baryonic and isospin chemical potentials are included in the hydrodynamic simulation, p/π^- ratio can slightly be changed in low p_T region: Baryon (isospin) chemical potential pushes up (down) proton yield from hydrodynamic components.

C. Elliptic flow for identified particles

Azimuthal asymmetry for noncentral heavy ion collisions is generally considered to be generated only by the final state interactions of matter created in the collisions. In hydrodynamic models, elliptic flow is created by the anisotropic initial configuration of high pressure matter which might be the QGP phase.
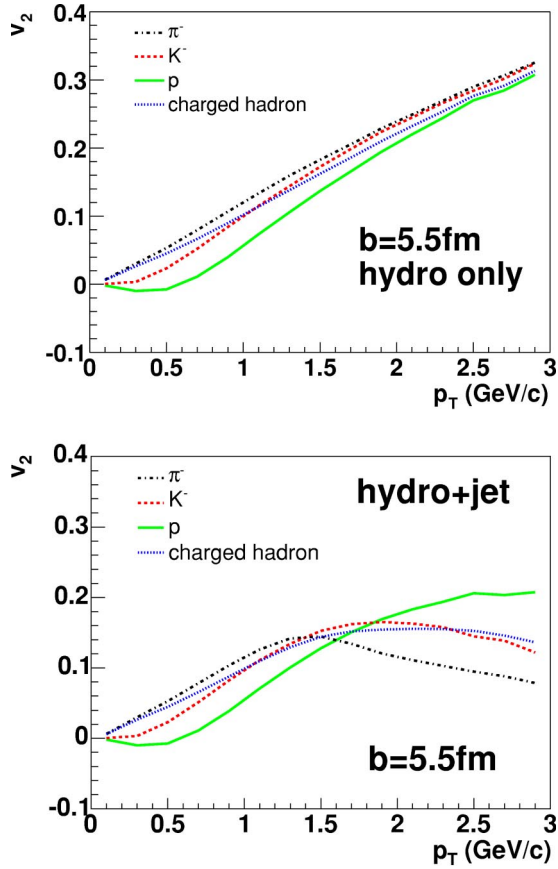
FIG. 9. (Color online) Transverse momentum dependence of the elliptic flow $v_2(p_T)$ for π^-, K^-, and p in Au+Au collisions at $\sqrt{s_{NN}}=200$ GeV at impact parameter $b=5.5$ fm from the hydrodynamic model (upper panel) and the hydro+jet model (lower panel). v_2 for charged hadrons are also represented in dotted lines.

Hydrodynamic predictions on the transverse momentum dependence of elliptic flow v_2 show almost linear increase for all particles. However, the experimental data saturate at high p_T [14,77,78]. More interestingly, pion v_2 is larger than that of protons at $p_T < 1$ GeV/c, while proton v_2 becomes larger than pion v_2 at some p_T [79]. Hydrodynamic calculations are successful in reproducing the mass dependence of the v_2 in the low transverse momentum region [26–29]. v_2 for pions are always greater than that of protons in hydrodynamics and, eventually, v_2 becomes almost mass independent at high transverse momenta as shown in Fig. 9. On the other hand, to understand the observed azimuthal asymmetry at large p_T, it was showed that the jet interaction with matter generates the azimuthal asymmetry for noncentral collisions [31,80,81].

We demonstrate in Fig. 9 that, by combining minijet components with hydrodynamics, pion v_2 can be reduced faster than proton v_2 at moderate high transverse momentum. The hydro+jet predictions on v_2 for identified particles in Au+Au collisions at RHIC for impact parameter $b=5.5$ fm are compared to hydro results in Fig. 9. The magnitude of v_2 for kaons and protons becomes larger than v_2 for pions at about $p_T > 1.3$ GeV/c. The shape of v_2 for pions saturates faster than those of kaons and protons, because the fraction of hydro components for pions are much smaller than that for

kaons or protons in this p_T region. This is again the consequence of radial flow effect. We demonstrate that the saturation point in transverse momentum depends on the hadron mass. As a whole effect of the sum of pions, kaons, and protons, the saturation point of v_2 for charged particles in transverse momentum is turned out to be $p_T=1.5$ GeV/c in our model at $b=5.5$ fm as one can read from Fig. 9.

Our semimacroscopic model produces consistent behavior in v_2 with the experimental data from PHENIX [79]. Recently, a microscopic description of quark coalescence model [23] shows the crossing of meson and baryon v_2's at $p_T \sim 1$ GeV/c. In the simple coalescence model where all partons have similar elliptic flow, elliptic flow for baryons roughly 1.5 times stronger than for mesons. On the other hand, our approach will have only mass dependence on the elliptic flow indicating $v_\Lambda \sim v_\phi$. Therefore, it is interesting to see, for example, ϕ meson elliptic flow to clarify the origin of the elliptic flow.

We have studied v_2 in the momentum range where both soft and hard contributions are important. It is interesting to see v_2 up to 10 GeV/c. Experimental data show that v_2 at high momentum saturates [77]. Systematic study on the elliptic flow within our model is under way including centrality as well as rapidity dependence.

IV. SUMMARY

We have studied the interplay of soft and hard components by looking at p_T spectra, suppression factors, hadron ratios, and elliptic flow for identified particles within the hydro+jet model. By taking into account both hydrodynamic radial flow and quenched pQCD spectra, it was found that $p_{T,\text{cross}}$, at which the yield from the soft component is identical to the one from the hard component, depends on the hadron species: $p_{T,\text{cross}} \sim 1.8$, 2.5, and 3.5 GeV/$c$ for pions, kaons, and protons in Au+Au central collisions at RHIC. This difference comes from the interplay between the radial flow for the soft part and the jet quenching for the hard part. From the consequences of the interplay between soft and hard hadronic components, we showed $p/\pi^- \sim 1$ and $R_{AA}(p_T) > 1$ at intermediate p_T for protons. We also showed that the mass dependence of the strength of $v_2(p_T)$ in the intermediate p_T region is also explained by the radial flow + pQCD components. Hydrodynamic radial flow plays an important role to understand the transverse dynamics when hadron mass is large.

[1] Nucl. Phys. **A698**, 1c (2002); **A715**, 1c (2003).

[2] M. Gyulassy and M. Plümer, Phys. Lett. B **243**, 432 (1990); X.-N. Wang and M. Gyulassy, Phys. Rev. Lett. **68**, 1480 (1992); M. Gyulassy and X.-N. Wang, Nucl. Phys. **B420**, 583 (1994); X.-N. Wang, M. Gyulassy, and M. Plümer, Phys. Rev. D **51**, 3436 (1995).

[3] M. Gyulassy, I. Vitev, X. N. Wang, and B. W. Zhang, nucl-th/0302077.

[4] R. Baier, Y. L. Dokshitzer, S. Peigné, and D. Schiff, Phys. Lett. B **345**, 277 (1995); R. Baier, Y. L. Dokshitzer, A. H. Mueller, S. Peigné, and D. Schiff, Nucl. Phys. **B484**, 265 (1997); R. Baier, Y. L. Dokshitzer, A. H. Mueller, and D. Schiff, Phys. Rev. C **58**, 1706 (1998); R. Baier, D. Schiff, and B. G. Zakharov, Annu. Rev. Nucl. Part. Sci. **50**, 37 (2000).

[5] U. A. Wiedemann, Nucl. Phys. **B588**, 303 (2000).

[6] B. G. Zakharov, JETP Lett. **63**, 952 (1996).

[7] M. Gyulassy, P. Lévai, and I. Vitev, Nucl. Phys. **B594**, 371 (2001); **B571**, 197 (2000); Phys. Rev. Lett. **85**, 5535 (2000).

[8] K. Adcox et al., Phys. Rev. Lett. **88**, 022301 (2002).

[9] S. S. Adler et al., Phys. Rev. Lett. **91**, 072301 (2003).

[10] C. Adler et al., Phys. Rev. Lett. **89**, 202301 (2002).

[11] J. Adams et al., Phys. Rev. Lett. **91**, 172302 (2003).

[12] K. Adcox et al., Phys. Lett. B **561**, 82 (2003).

[13] S. S. Adler et al., Phys. Rev. Lett. **91**, 172301 (2003).

[14] P. Sorensen et al., nucl-ex/0305008; J. Adams et al., Phys. Rev. Lett. **92**, 052302 (2004).

[15] I. Vitev and M. Gyulassy, Phys. Rev. Lett. **89**, 252301 (2002); X. N. Wang, nucl-th/0305010.

[16] X. F. Zhang, G. Fai, and P. Levai, Phys. Rev. Lett. **89**, 272301 (2002).

[17] I. Vitev and M. Gyulassy, Nucl. Phys. **A715** 779, 2003; Phys. Rev. C **65**, 041902 (2002).

[18] V. Topor Pop, M. Gyulassy, J. Barrette, C. Gale, S. E. Vance, X. N. Wang, N. Xu, and K. Filimonov, Phys. Rev. C **68**, 054902 (2003).

[19] Z. W. Lin and C. M. Ko, Phys. Rev. C **65**, 034904 (2002); Z. W. Lin, C. M. Ko, and S. Pal, Phys. Rev. Lett. **89**, 152301 (2002).

[20] R. C. Hwa and C. B. Yang, Phys. Rev. C **67**, 034902 (2003).

[21] R. J. Fries, B. Muller, C. Nonaka, and S. A. Bass, Phys. Rev. Lett. **90**, 202303 (2003); Phys. Rev. C **68**, 044902 (2003).

[22] V. Greco, C. M. Ko, and P. Levai, Phys. Rev. Lett. **90**, 202302 (2003); Phys. Rev. C **68**, 034904 (2003).

[23] D. Molnar and S. A. Voloshin, Phys. Rev. Lett. **91**, 092301 (2003); Z. W. Lin and D. Molnar, Phys. Rev. C **68**, 044901 (2003); D. Molnar, J. Phys. G **30**, 5235 (2004).

[24] S. J. Casalderrey and E. V. Shuryak, hep-ph/0305160.

[25] T. Peitzmann, Nucl. Phys. **A727**, 179 2003.

[26] P. F. Kolb, P. Huovinen, U. Heinz, and H. Heiselberg, Phys. Lett. B **500**, 232 (2001); P. Huovinen, P. F. Kolb, U. W. Heinz, P. V. Ruuskanen, and S. A. Voloshin, ibid. **503**, 58 (2001); P. F. Kolb, U. W. Heinz, P. Huovinen, K. J. Eskola, and K. Tuominen, Nucl. Phys. **A696**, 197 (2001).

[27] D. Teaney, J. Lauret, and E. V. Shuryak, Phys. Rev. Lett. **86**, 4783 (2001); nucl-th/0110037.

[28] T. Hirano, Phys. Rev. C **65**, 011901 (2002).

[29] T. Hirano and K. Tsuda, Phys. Rev. C **66**, 054905 (2002).

[30] P. Huovinen, nucl-th/0305064; P. F. Kolb and U. Heinz, nucl-th/0305084.

[31] M. Gyulassy, I. Vitev, and X. N. Wang, Phys. Rev. Lett. **86**, 2537 (2001).

[32] M. Gyulassy, I. Vitev, X. N. Wang, and P. Huovinen, Phys. Lett. B **526**, 301 (2002).

[33] E. Wang and X. N. Wang, Phys. Rev. C **64**, 034901 (2001).

[34] T. Hirano and Y. Nara, Phys. Rev. C **66**, 041901(R) (2002).

[35] T. Sjostrand, P. Eden, C. Friberg, L. Lonnblad, G. Miu, S. Mrenna, and E. Norrbin, Comput. Phys. Commun. **135**, 238 (2001).

[36] U. W. Heinz and P. F. Kolb, hep-ph/0204061.

[37] K. J. Eskola, P. V. Ruuskanen, S. S. Rasanen, and K. Tuominen, Nucl. Phys. **A696**, 715 (2001).

[38] T. Hirano and Y. Nara, Phys. Rev. Lett. **91**, 082301 (2003).

[39] C. Adler et al., Phys. Rev. Lett. **90**, 082302 (2003).

[40] L. D. McLerran, Lect. Notes Phys. **583**, 291 (2002); E. Iancu, A. Leonidov, and L. McLerran, hep-ph/0202270; E. Iancu and R. Venugopalan, hep-ph/0303204.

[41] R. Baier, A. H. Mueller, D. Schiff, and D. T. Son, Phys. Lett. B **502**, 51 (2001); **539**, 46 (2002).

[42] J. Sollfrank, P. Huovinen, M. Kataja, P. V. Ruuskanen, M. Prakash, and R. Venugopalan, Phys. Rev. C **55**, 392 (1997).

[43] I. G. Bearden et al., Phys. Rev. Lett. **90**, 102301 (2003).

[44] See, for example, E. V. Shuryak, Nucl. Phys. **A661**, 119c (1999); U. W. Heinz, ibid. **A661**, 140c (1999).

[45] N. Arbex, F. Grassi, Y. Hama, and O. Socolowski, Phys. Rev. C **64**, 064906 (2001).

[46] D. Teaney, nucl-th/0204023.

[47] P. F. Kolb and R. Rapp, Phys. Rev. C **67**, 044903 (2003).

[48] T. Hirano and Y. Nara, Nucl. Phys. **A721**, 277 (2003).

[49] F. Cooper and G. Frye, Phys. Rev. D **10**, 186 (1974).

[50] I. G. Bearden et al., BRAHMS Collaboration, Phys. Rev. Lett. **88**, 202301 (2002).

[51] P. Huovinen, Nucl. Phys. **A715**, 299c (2003).

[52] It is often said that the multiplicity scales with the number of participants, not binary collision. This does not mean that the initial energy scales with the number of participants, since the energy itself is not directly proportional to the final multiplicity of hadrons. There is also so-called pdV work during expansion, hence dE/dy is not a conserved number. The behavior of centrality is consistent with previous work. See, e.g., the last paper in Ref. [26].

[53] V. Emel'yanov, A. Khodinov, S. R. Klein, and R. Vogt, Phys. Rev. C **61**, 044904 (2000).

[54] K. J. Eskola, V. J. Kolhinen, and P. V. Ruuskanen, Nucl. Phys. **B535**, 351 (1998); K. J. Eskola, V. J. Kolhinen, and C. A. Salgado, Eur. Phys. J. C **9**, 61 (1999).

[55] J. W. Cronin, H. J. Frisch, M. J. Shochet, J. P. Boymond, P. A. Piroué, and R. L. Sumner, Phys. Rev. D **11**, 3105 (1975); D. Antreasyan, J. W. Cronin, H. J. Frisch, M. J. Shochet, L. Kluberg, P. A. Piroue, and R. L. Sumner, ibid. **19**, 764 (1979).

[56] B. B. Back et al., Phys. Rev. Lett. **91**, 072302 (2003); S. S. Adler et al., ibid. **91**, 072303 (2003); J. Adams et al., ibid. **91**, 072304 (2003); I. Arsene et al., ibid. **91**, 072305 (2003).

[57] X. N. Wang, Phys. Rev. C **61**, 064910 (2000); Phys. Lett. B **565**, 116 (2003).

[58] A. Dumitru and J. Jalilian-Marian, Phys. Rev. Lett. **89**, 022301 (2002); , Phys. Lett. B **547**, 15 (2002); F. Gelis and J. Jalilian-Marian, Phys. Rev. D **66**, 014021 (2002).

[59] A. Accardi, Phys. Lett. B **577**, 54 (2003); I. Vitev, Phys. Lett. B **562**, 36 (2003); P. Levai, G. Papp, G. G. Barnafoldi, and G. Fai, nucl-th/0306019; R. Baier, A. Kovner, and U. A. Wiede-

mann, Phys. Rev. D **68**, 054009 (2003); D. Kharzeev, Y. V. Kovchegov, and K. Tuchin, *ibid.* **68**, 094013 (2003); J. Jalilian-Marian, Y. Nara, and R. Venugopalan, nucl-th/0307022.

[60] S. S. Adler *et al.*, Phys. Rev. Lett. **91**, 241803 (2003).

[61] H. L. Lai *et al.*, Eur. Phys. J. C **12**, 375 (2000).

[62] J. Adams *et al.*, nucl-ex/0309012.

[63] P. Aurenche, M. Fontannaz, J. P. Guillet, B. A. Kniehl, E. Pilon, and M. Werlen, Eur. Phys. J. C **9**, 107 (1999); P. Aurenche, M. Fontannaz, J. P. Guillet, B. A. Kniehl, and M. Werlen, *ibid.* **13**, 347 (2000). The code is available from http://wwwlapp.in2p3.fr /lapth/PHOX_FAMILY/main.html

[64] A. D. Martin, R. G. Roberts, W. J. Stirling, and R. S. Thorne, Eur. Phys. J. C **14**, 133 (2000).

[65] B. A. Kniehl, G. Kramer, and B. Potter, Nucl. Phys. **B582**, 514 (2000).

[66] S. Kretzer, Phys. Rev. D **62**, 054001 (2000). Proton fragmentation function itself is not represented in this paper. Here we assume that protons are obtained by subtracting pions and kaons from positive charged hadrons.

[67] J. D. Bjorken, Phys. Rev. D **27**, 140 (1983).

[68] Parton density $\rho(\tau,x)$ from our full three-dimensional hydrodynamic simulation used in this paper and Ref. [38] can be downloaded on the web: http://quark.phy.bnl.gov/~hirano/hydrodata/par_evo.html; the package includes a sample FORTRAN program which calls local parton density, temperature, and transverse velocity in the QGP phase.

[69] We used $C=0.35$ in the previous paper [38] in which neither nuclear shadowing effects nor impact parameter dependent intrinsic k_T is included. We note that our results for back-to-back correlations are the same after inclusion of nuclear shadowing and impact parameter dependent intrinsic k_T.

[70] L. D. Landau and I. P. Pomeranchuk, Dokl. Akad. Nauk SSSR, Ser. A **92**, 535 (1953); **92**, 735 (1953); A. B. Migdal, Phys. Rev. **103**, 1811 (1956).

[71] L. D. McLerran and R. Venugopalan, Phys. Rev. D **49**, 2233 (1994); **49**, 3352 (1994); **50**, 2225 (1994).

[72] E. V. Shuryak and I. Zahed, Phys. Rev. D **67**, 054025 (2003).

[73] A. Krasnitz and R. Venugopalan, Nucl. Phys. **B557**, 237 (1999); Phys. Rev. Lett. **86**, 1717 (2001); **84**, 4309 (2000); A. Krasnitz, Y. Nara, and R. Venugopalan, *ibid.* **87**, 192302 (2001); Nucl. Phys. **A717**, 268 (2003); **A727**, 427 (2003).

[74] S. S. Adler *et al.*, nucl-ex/0307022.

[75] T. S. Biro, P. Levai, and J. Zimanyi, Phys. Lett. B **347**, 6 (1995); J. Zimanyi, T. S. Biro, T. Csorgo, and P. Levai, Heavy Ion Phys. **4**, 15 (1996).

[76] P. Csizmadia and P. Levai, Phys. Rev. C **61**, 031903 (2000).

[77] C. Adler *et al.*, Phys. Rev. Lett. **90**, 032301 (2003).

[78] S. Manly *et al.*, Nucl. Phys. **A715**, 611 (2003).

[79] S. S. Adler *et al.*, Phys. Rev. Lett. **91**, 182301 (2003).

[80] X. N. Wang, Phys. Rev. C **63**, 054902 (2001).

[81] E. V. Shuryak, Phys. Rev. C **66**, 027902 (2002).